

Modeling of the Hysteretic Behavior of Wire Rope Isolators Using a Novel Rate-Independent Model



Nicolò Vaiana, Francesco Marmo, Salvatore Sessa, and Luciano Rosati

Abstract This paper presents a novel rate-independent model to predict the hysteretic response of Wire Rope Isolators along their two principal transverse directions, namely Roll and Shear directions. Employing the proposed model, the device restoring force can be evaluated by solving an algebraic equation that requires a set of only five parameters directly related to specific graphical features of the hysteresis loop. To verify such a model, some experimental results, obtained during several experimental tests recently performed at the Department of Industrial Engineering of the University of Naples Federico II, are predicted analytically.

Keywords Wire rope isolator · Hysteretic behavior · Rate-independent model

1 Introduction

Wire Rope Isolators are devices manufactured by embedding a stainless steel cable, having a helix shape, into two metal retainer bars [1].

These devices generally exhibit a kinematic hardening hysteretic behavior when a displacement time history is applied along one of their two principal transverse directions, denominated Roll and Shear directions, respectively. Indeed, the distance between the two parallel curves, that typically limit their hysteresis loops, remains constant during the entire deformation process and the device restoring force increases when a transverse displacement with increasing amplitude is applied.

Several differential rate-independent models are currently available in the literature to accurately reproduce the complex transverse response characterizing such metal devices [2–6]. Unfortunately, these phenomenological models suffer from some limitations such as the unclear mechanical significance of the adopted

N. Vaiana (✉) · F. Marmo · S. Sessa · L. Rosati
Department of Structures for Engineering and Architecture,
University of Naples Federico II, Naples, Italy
e-mail: nicolo.vaiana@unina.it

parameters and the limited computational efficiency due to the need of numerically solving a differential equation to predict the device response.

This paper presents a novel rate-independent model, formulated by specializing a general class of models recently proposed by Vaiana et al. [7–9], to reproduce the response of Wire Rope Isolators along the Roll and Shear directions. In particular, this model offers several advantages, such as the use of a small number of parameters, which have a precise mechanical significance, as well as a significant computational efficiency due to the solution of an algebraic equation, rather than a differential one, to compute the device restoring force.

2 Proposed Hysteretic Model

The Proposed Hysteretic Model (PHM) has been formulated by specializing a recently developed family of uniaxial models [7–9].

Such a general formulation assumes the generalized displacement u (generalized rate-independent hysteretic force f_{ri}) as input (output) variable, and describes a generalized rate-independent force-displacement hysteresis loop by adopting four different curves: the upper c_u and the lower c_l limiting curves and the generic loading c^+ and unloading c^- curves.

Figure 1 illustrates the four curves describing a hysteresis loop limited by two parallel curves; note that the generic loading (unloading) curve, defined by a positive (negative) sign of the generalized velocity \dot{u} , is identified by an arrow plotted on the curve.

As shown in Fig. 1, the upper (lower) limiting curve intersects the vertical axis at the point with coordinates 0 and \bar{f} ($-\bar{f}$). Furthermore, the generic loading (unloading) curve intersects the lower (upper) limiting curve at a point having

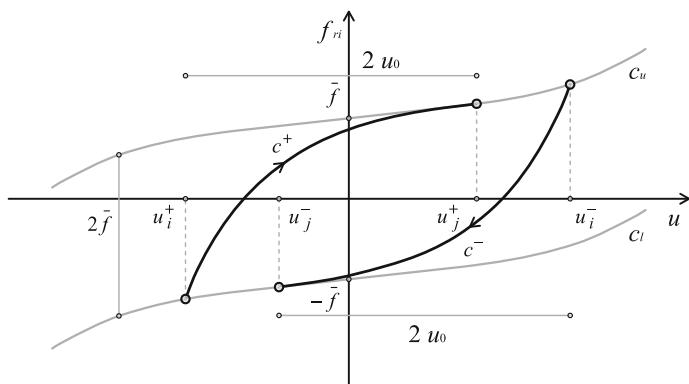


Fig. 1 An example of hysteresis loop described by the curves c_u , c_l , c^+ , and c^-

abscissa u_i^+ (u_i^-), and the upper (lower) limiting curve at a point having abscissa u_j^+ (u_j^-), with $u_i^+ = u_j^+ - 2u_0$ ($u_i^- = u_j^- + 2u_0$).

In the following subsections, we first describe the PHM formulation by introducing the proposed expressions of the generalized rate-independent hysteretic force and of the history variable; then, we show how each PHM parameter affects the size and/or the shape of a hysteresis loop.

2.1 PHM Formulation

The PHM requires the calibration of only five parameters, that is, k_a , k_b , α , β_1 , and β_2 . In addition, it also adopts two additional parameters, namely $u_0 > 0$ and $\bar{f} > 0$, that can be computed after selecting k_a , k_b , α taking into account the following conditions: $k_a > k_b$, $k_a > 0$, $\alpha > 0$, and $\alpha \neq 1$.

2.1.1 Generalized Rate-Independent Force

According to Fig. 1, during a generic loading (unloading) phase, $f_{ri} = c^+$ ($f_{ri} = c^-$) if $u_i^+ \leq u < u_j^+$ ($u_j^- < u \leq u_i^-$), whereas $f_{ri} = c_u$ ($f_{ri} = c_l$) if $u > u_j^+$ ($u < u_j^-$).

In particular, in the PHM, the expressions of c_u and c_l are

$$c_u(u) = \beta_1 u^3 + \beta_2 u^5 + k_b u + \bar{f}, \tag{1}$$

$$c_l(u) = \beta_1 u^3 + \beta_2 u^5 + k_b u - \bar{f}, \tag{2}$$

whereas the ones of c^+ and c^- are

$$c^+(u, u_j^+) = \beta_1 u^3 + \beta_2 u^5 + k_b u + (k_a - k_b) \left[\frac{(1 + u - u_j^+ + 2u_0)^{(1-\alpha)}}{1 - \alpha} - \frac{(1 + 2u_0)^{(1-\alpha)}}{1 - \alpha} \right] + \bar{f}, \tag{3}$$

$$c^-(u, u_j^-) = \beta_1 u^3 + \beta_2 u^5 + k_b u + (k_a - k_b) \left[\frac{(1 - u + u_j^- + 2u_0)^{(1-\alpha)}}{\alpha - 1} - \frac{(1 + 2u_0)^{(1-\alpha)}}{\alpha - 1} \right] - \bar{f}. \tag{4}$$

Furthermore, the expression of \bar{f} , required in Eqs. (1)–(4), is

$$\bar{f} = \frac{k_a - k_b}{2} \left[\frac{(1 + 2u_0)^{(1-\alpha)} - 1}{1 - \alpha} \right]. \tag{5}$$

Since $k_a > k_b$, $\alpha \neq 1$, and $u_0 > 0$, Eq. (5) gives a positive value of \bar{f} .

2.1.2 History Variable

In the PHM, the expression of u_j^+ is

$$u_j^+ = 1 + u_P + 2u_0 - \left\{ \frac{1 - \alpha}{k_a - k_b} \left[f_P - \beta_1 u_P^3 - \beta_2 u_P^5 - k_b u_P - \bar{f} + (k_a - k_b) \frac{(1 + 2u_0)^{(1-\alpha)}}{1 - \alpha} \right] \right\}^{\left(\frac{1}{1-\alpha}\right)}, \tag{6}$$

whereas the one of u_j^- is

$$u_j^- = -1 + u_P - 2u_0 + \left\{ \frac{\alpha - 1}{k_a - k_b} \left[f_P - \beta_1 u_P^3 - \beta_2 u_P^5 - k_b u_P + \bar{f} + (k_a - k_b) \frac{(1 + 2u_0)^{(1-\alpha)}}{\alpha - 1} \right] \right\}^{\left(\frac{1}{1-\alpha}\right)}. \tag{7}$$

2.2 Parameter Sensitivity Analysis

Figure 2 shows how the size and (or) the shape of hysteresis loops, obtained by imposing a full sinusoidal cycle of generalized displacement having amplitude of 1, change(s) due to the variation of each PHM parameter. In particular, it can be noted that:

- k_a affects the hysteresis loop size (Fig. 2a);
- k_b produces a rotation of the hysteresis loop and a slight variation of its size (Fig. 2b);
- α affects the hysteresis loop size (Fig. 2c);
- β_1 affects the hysteresis loop shape (Fig. 2d).

Since the variation of the hysteresis loop shape due to β_2 is similar to the one produced by β_1 , the related figure is not presented for brevity.

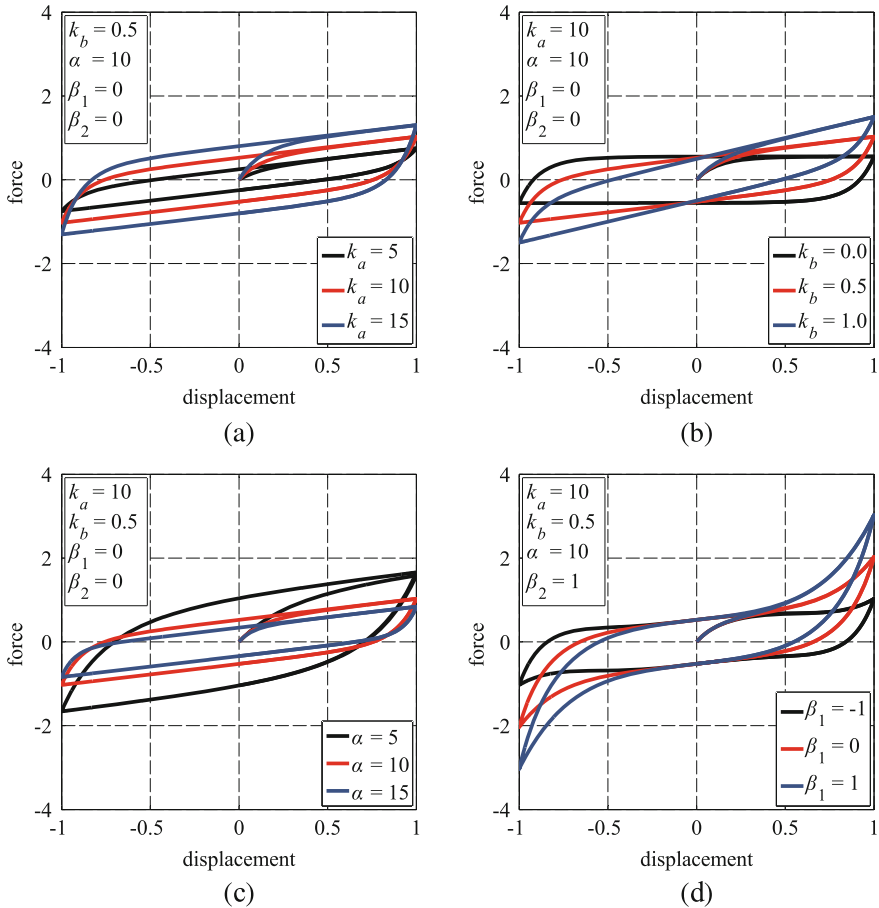


Fig. 2 Variation of the hysteresis loop size and/or shape associated with each PHM parameter

3 Experimental Verification

In this section the PHM, illustrated in Sect. 2, is validated by comparing the analytical results with those obtained from several dynamic tests performed on a Wire Rope Isolator (WRI) at the Department of Industrial Engineering of the University of Naples Federico II (Italy) by Vaiana et al. [10].

3.1 Tested Wire Rope Isolator

Figure 3a shows the geometrical characteristics of the tested WRI having two principal transverse directions, denominated Roll and Shear directions. Such a metal

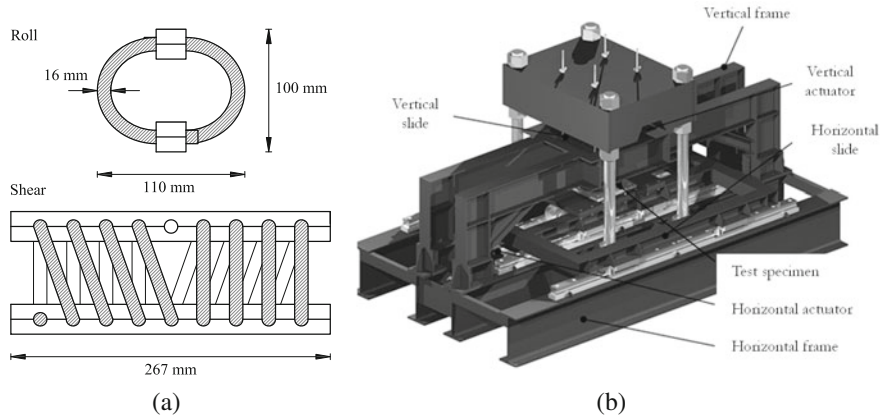


Fig. 3 Tested wire rope isolator (a) and adopted testing machine (b)

device, manufactured by Powerflex S.r.l. (Limatola, Italy), has been constructed by assembling two types of elements: a Stainless Steel Type 316 wire rope and two aluminum alloy retainer bars. Specifically, the wire rope, constituted by six strands wrapped around a central one, has been wound in the shape of a helix and embedded into the two retainer bars. Each external strand of the wire rope is made of 25 steel wires, whereas the inner one is made of 49 steel wires.

Figure 3b shows the Testing Machine (TM) adopted to perform the experimental tests. Such a machine allows one to impose a transverse displacement or force, by means of a horizontal hydraulic actuator, under the effect of a constant axial compressive force, applied by means of a vertical hydraulic actuator [11–13]. The tested WRI has been installed by fixing its retainer bars to the lower and upper rigid steel plates of the TM.

During the experimental tests, conducted at room temperature, the time history of the relative transverse displacement between the TM lower and upper plates and the time histories of the axial and transverse forces have been measured by sampling the data at 250 Hz.

3.2 Simulation of the Experimental Behavior

Figure 4 (5) illustrates both the analytical and experimental hysteresis loops that have been obtained by imposing, to the tested WRI, five cycles of sinusoidal transverse displacement, having frequency of 1 Hz; in particular, such results have been obtained for three different amplitude levels, that is, 0.25, 0.50, and 1 cm, and by applying a constant axial compressive force, f_v , of 0 kN (2 kN). Note that Figs. 4a and 5a show the results along the Roll direction, whereas Figs. 4b and 5b present the results along the Shear direction.

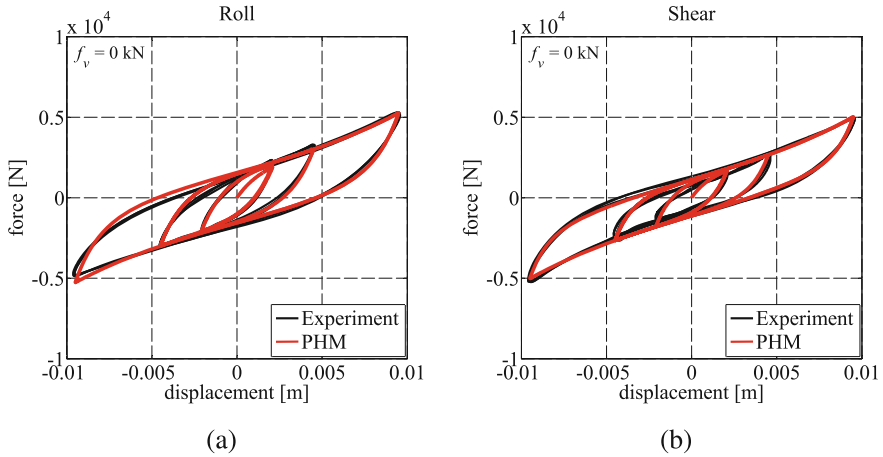


Fig. 4 Analytical and experimental hysteresis loops obtained in roll (a) and shear (b) directions for $f_v = 0$ kN

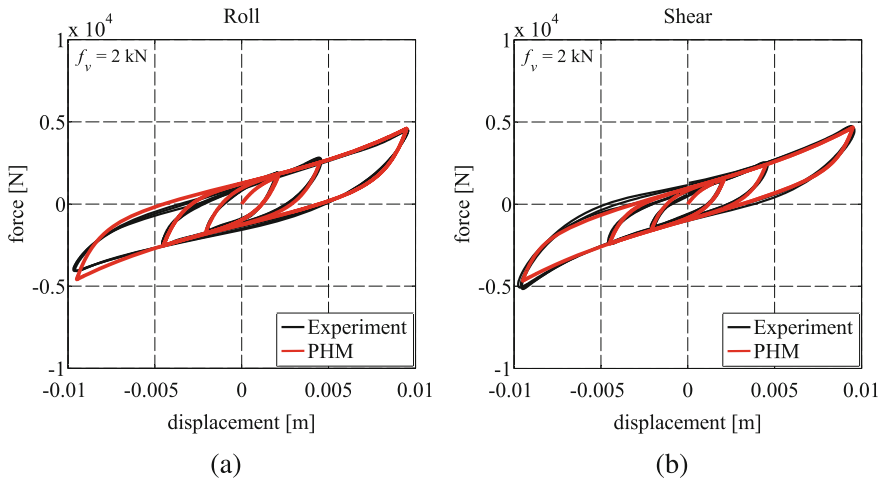


Fig. 5 Analytical and experimental hysteresis loops obtained in roll (a) and shear (b) directions for $f_v = 2$ kN

A satisfactory agreement can be observed between the experimental hysteresis loops and the analytical ones, simulated by adopting the PHM parameters listed in Table 1 (2). Such model parameters have been calibrated through a simple analytical fitting of the experimental data. Note that, although in this case it has been possible setting $\beta_2 = 0$, all five model parameters are typically required for accuracy reasons.

Thus, it has been demonstrated that the PHM can well reproduce the stiffening behavior occurring in the tested WRI and that it requires only one set of parameters

Table 1 PHM parameters used for reproducing the hysteresis loops in Fig. 4

$f_v = 0$ kN	k_a [Nm ⁻¹]	k_b [Nm ⁻¹]	α	β_1 [Nm ⁻³]	β_2 [Nm ⁻⁵]
(a) Roll	28×10^5	30×10^4	8×10^2	10×10^8	0
(b) Shear	28×10^5	32×10^4	11×10^2	10×10^8	0

Table 2 PHM parameters used for reproducing the hysteresis loops in Fig. 5

$f_v = 2$ kN	k_a [Nm ⁻¹]	k_b [Nm ⁻¹]	α	β_1 [Nm ⁻³]	β_2 [Nm ⁻⁵]
(a) Roll	28×10^5	26×10^4	10×10^2	10×10^8	0
(b) Shear	28×10^5	30×10^4	13×10^2	10×10^8	0

to simulate the device response obtained at various levels of amplitude in the presence of a constant axial compressive force.

Finally, the comparison of Tables 1 and 2 shows that the set of model parameters has to be suitably calibrated, based on the experimental results, in order to account for a different value of the applied constant axial compressive force.

4 Conclusions

We have illustrated a novel rate-independent model capable of predicting the hysteretic response of WRIs along their Roll and Shear transverse directions in the presence of a constant axial compressive force.

Adopting the PHM, the device restoring force can be computed by solving an algebraic equation requiring a set of only five parameters which are characterized by a clear mechanical significance, as shown in Sect. 2.2.

According to the experimental verification, it can be concluded that:

- the WRIs hysteretic behavior obtained at various amplitude levels, including the stiffening behavior, can be simulated by means of the PHM using only one set of parameters;
- the WRIs hysteretic behavior obtained for a different value of the constant axial compressive force can be simulated by conveniently recalibrating the set of five model parameters.

Forthcoming papers will show the numerical accuracy as well as the computational efficiency of the PHM by performing nonlinear time history analyses [14] on hysteretic mechanical systems and comparing the results with those obtained by using the celebrated Bouc–Wen model [15, 16] or its modified version [3, 4].

References

1. Ko, J.M., Ni, Y.Q., Tian, Q.L.: Hysteretic behavior and empirical modeling of a wire-cable vibration isolator. *Int. J. Anal. Exp. Modal Anal.* **7**(2), 111–127 (1992)
2. Demetriades, G.F., Constantinou, M.C., Reinhorn, A.M.: Study of wire rope systems for seismic protection of equipment in buildings. *Eng. Struct.* **15**(5), 321–334 (1993)
3. Ni, Y.Q., Ko, J.M., Wong, C.W., Zhan, S.: Modelling and identification of a wire-cable vibration isolator via a cyclic loading test. Part 1: experiments and model development. *J. Syst. Control Eng.* **213**(3), 163–171 (1999)
4. Ni, Y.Q., Ko, J.M., Wong, C.W., Zhan, S.: Modelling and identification of a wire-cable vibration isolator via a cyclic loading test. Part 2: identification and response prediction. *J. Syst. Control Eng.* **213**(3), 173–182 (1999)
5. Wang, H-X., Gong, X-S., Pan, F., Dang, X-J.: Experimental investigations on the dynamic behaviour of O-type wire-cable vibration isolators. *Shock Vib.* **2015**, Article ID 869325, 12 pp. (2015)
6. Chang, C-M., Strano, S., Terzo, M.: Modelling of hysteresis in vibration control systems by means of the Bouc-Wen model. *Shock Vib.* **2016**, Article ID 3424191, 14 pp. (2016)
7. Vaiana, N., Sessa, S., Marmo, F., Rosati, L.: A class of uniaxial phenomenological models for simulating hysteretic phenomena in rate-independent mechanical systems and materials. *Nonlinear Dyn.* **93**(3), 1647–1669 (2018)
8. Vaiana, N., Sessa, S., Marmo, F., Rosati, L.: An accurate and computationally efficient uniaxial phenomenological model for steel and fiber reinforced elastomeric bearings. *Compos. Struct.* **211**, 196–212 (2019)
9. Vaiana, N., Sessa, S., Marmo, F., Rosati, L.: Nonlinear dynamic analysis of hysteretic mechanical systems by combining a novel rate-independent model and an explicit time integration method. *Nonlinear Dyn.* (2019). <https://doi.org/10.1007/s11071-019-05022-5>
10. Vaiana, N., Spizzuoco, M., Serino, G.: Wire rope isolators for seismically base-isolated lightweight structures: experimental characterization and mathematical modeling. *Eng. Struct.* **140**, 498–514 (2017)
11. Strano, S., Terzo, M.: Actuator dynamics compensation for real-time hybrid simulation: an adaptive approach by means of a nonlinear estimator. *Nonlinear Dyn.* **85**(4), 2353–2368 (2016)
12. Losanno, D., Madera Sierra, I.E., Spizzuoco, M., Marulanda, J., Thomson, P.: Experimental assessment and analytical modeling of novel fiber-reinforced isolators in unbounded configuration. *Compos. Struct.* **212**, 66–82 (2019)
13. Madera Sierra, I.E., Losanno, D., Strano, S., Marulanda, J., Thomson, P.: Development and experimental shear behavior of HDR seismic isolators for low-rise residential buildings. *Eng. Struct.* **183**, 894–906 (2019)
14. Greco, F., Luciano, R., Serino, G., Vaiana, N.: A mixed explicit-implicit time integration approach for nonlinear analysis of base-isolated structures. *Annals Solid Struct. Mech.* **10**, 17–29 (2018)
15. Bouc, R.: Modele mathematique d'hysteresis. *Acustica* **24**, 16–25 (1971)
16. Wen, Y.K.: Method for random vibration of hysteretic systems. *J. Eng. Mech. Div. ASCE* **102**(2), 249–263 (1976)